Separation and Purification Technology xxx (xxxx) xxxx

Contents lists available at ScienceDirect

Separation and Purification Technology

journal homepage: www.elsevier.com/locate/seppur

Optimization of polymeric nanofiltration performance for olive-oil-washing wastewater phenols recovery and reclamation

J.M. Ochando-Pulido*, J.R. Corpas-Martínez, J.A. Vellido-Perez, A. Martinez-Ferez

Department of Chemical Engineering, University of Granada, Avenida Fuentenueva s/n, 18071 Granada, Spain

ARTICLE INFO

Keywords:
Olive-oil-washing wastewater
Fouling
Nanofiltration
Threshold flux
Wastewater reclamation

ABSTRACT

The core of the present work was to model and optimize an environmentally friendly nanofiltration (NF) treatment process for two-phase olive-oil-washing wastewater (OOWW) valorization throughout the concentration and recovery of its phenolic fraction and the obtention of a purified permeate stream. For this objective, a factorial design was used for the optimization of the process. Results were interpreted by means of the response surface methodology. A statistical multifactorial analysis was performed in order to quantify all the potential complex conjugated effects of the input parameters in the NF process. The process was subsequently modelled by means of a second-grade quadratic fitting model equation. Finally, the parametric quality standards that permit to reuse the purified stream for irrigation, recycling or even discharge in-site reuse purposes were checked. To the author's knowledge, no previous work on the optimization and statistical modelling of membrane processes for OOWW purification and valorization can be found up to the present. The optimized parameters for the proposed OOWW purification process – operating pressure of 26.5 bar, tangential velocity 32.7 $m\,s^{-1}$, system temperature 35 °C and pH of 3.7 – ensured high and stable membrane flux (106.2 $L\,h^{-1}\,m^{-2}$). The obtained optimized data are very relevant for the feasible scale-up of the proposed process in the mills, since the NF membrane (TFC polyamide/polysulfone, MWCO 300 Da) was highly efficient at ambient temperature conditions and raw effluent pH. The optimized conditions provided a permeate stream that could be reused for irrigation purposes and a retantate stream concentrated in volume up to 6.5 times, with a total phenolic content of minimum 1315.7 mg/L.

1. Introduction

Industrial wastewaters are, in general terms, liquid wastes of industrial origin that contain suspended, colloidal and/or dissolved (organic and inorganic) solids of chemical and/or biological nature. These effluents contain substances that, because of their nature or concentration, cannot be removed by conventional treatments applied to urban wastewaters. On the other hand, due to their toxicity or long-term biological effects, many of them are subjected to specific regulations. All this means that, in many cases, the treatment and management of these wastewaters constitute a management problem and concern for the industrial sector.

Focusing on the case of Spain – in general, in the Mediterranean region – olive oil industry is one of the most affected by the problem concerning wastewater treatment. In numbers, a medium-sized oil mill can currently produce 10–15 m^3 of wastewater per day from the olive oil vertical centrifugation, called olive-oil-washing wastewater (OOWW). That supposes a total volume of several millions of cubic meters of these contaminant effluents per year [1–6]. OOWW is a heavy-polluted agro-industrial effluent with high toxicity for aquatic fauna and flora. It is an environmental threat that is causing soil contamination, underground leakage and groundwater pollution in many regions [7–9]. The reason for this is found in its composition: OOWW contains, in addition to a wide range of organic contaminants, high concentrations of polyphenolic compounds that are responsible for the antimicrobial and phytotoxic actions and their difficult degradation under normal conditions [10]. Because of this, decades ago the different producing countries banned the dumping of olive mill wastewaters (OMW) into rivers and public waterways. Since then, oil mills are looking for methods to decontaminate these effluents before they are

Abbreviations: NF, nanofiltration; UF, ultrafiltration; OOWW, olive-oil-washing wastewater; OMW, olive mill wastewater; OMSW, olive mill solid waste; PZC, point of zero charge; VCF, volume concentration factor; ANOVA, analysis of variance; RSM, response surface methodology; N_{Re}, Reynolds number; R, hydraulic radius (m); A, area (m^2); P, pressure; T, temperature; F, feed flow; v_t, tangential velocity; ρ, fluid density (kg/m^3); μ, fluid viscosity (kg/m s); Jp, permeate flux (L/h m^2)

* Corresponding author.
E-mail address: jmochandop@ugr.es (J.M. Ochando-Pulido).

https://doi.org/10.1016/j.seppur.2019.116261
Received 24 July 2019; Received in revised form 19 October 2019; Accepted 25 October 2019
1383-5866/

discharged into the natural environment. Among the different methods proposed we can find disposal of OOWW by natural evaporation, oxidation, treatment with lime, agricultural soils, thermal concentration, composting and biological treatments [11].

Natural evaporation has been the most widely implemented method in the last decades [5]. Oil mills have built large artificial lagoons where they can deposit these residues and take advantage of solar energy and the favorable climatic conditions of these regions for their evaporation. After most of the water has been evaporated, the concentrated pollutant compounds remain at the bottom of the ponds, from where they are collected and taken to treatment plants for their total disposal. However, although this has been the most used method during all these years, it presents important limitations:

- This method is quite slow and inefficient, subjected to weather conditions at all times.
- Seasonality of olive-oil industry – which has a high production concentrated in a short period of time (November-February) – together with what we mentioned in the previous point, leads, in many cases, to the lack of capacity of artificial lagoons [12]. The construction of new and larger ponds to solve this problem entails investments for the acquisition of new land, conditioning thereof, construction and maintenance costs, etc.
- Artificial lagoons must be properly conditioned and fenced to avoid any type of accident: no animal, child or person can fall inside and die drowned.
- Artificial lagoons are associated with a visual impact, environmentally speaking, that remains even after the cessation of activity.
- Concentrated pollutant compounds that remain at the bottom of the ponds are degraded over time and produce strong bad odors.
- Finally, we cannot ignore the risk of leaks and overflows. Although artificial lagoons are covered with plastics and waterproofed, they deteriorate over time, end up breaking and causing spill with the consequent environmental damage that this entails.

Therefore, natural evaporation and artificial lagoons are merely provisional solutions, while exploring other safe and viable alternatives, more economical in the medium and long-term and more environmentally sustainable, should be encouraged. Among these possible alternatives, membrane technology stands out [13–16].

In the last years, nanofiltration (NF) and ultrafiltration (UF) membranes have been increasingly implemented by all type of industries for the treatment of their wastewaters, replacing the most conventional separation processes – generally quite inefficient, complex and, in many cases, too expensive. UF membranes are often used as secondary treatment to reduce the concentration of high-molecular-weight organic compounds, macromolecules and microorganisms, whereas NF membranes are tailored as tertiary treatments for the removal of dissolved inorganic compounds, low-molecular-weight organic matter and micropollutants [17].

NF membranes technology offers many benefits such as higher selectivity, lower energy consumption, higher efficiencies, no additives required, no phase changes and lower costs. All these advantages over conventional processes position it as an interesting and feasible alternative for this type of applications in which the final costs of purification are fundamental – the final product, purified water, is a product with a very low added value, with higher priority regarding social and environmental responsibility and legal requirements than the interest of the obtained product. Nevertheless, fouling is again mentioned as the most important limiting factor for the application of membrane technology for wastewaters treatment [18]. Fouling leads to a reduction of productivity over time, and in turn, may cause a remarkable shortening of the life-time of membrane modules [19–24]. Besides, fouling also affects the membrane selectivity and thus the rejection efficiency. The presence of significant fouling can make the process unsustainable from an economic point of view, but by controlling membrane fouling, the membrane may work for years without service shut-down, reducing the operating costs and the need for membrane substitution [6]. Hence, membrane process designers should avoid membrane fouling by operating membranes away from critical permeate flux point.

In this framework, predicting the performance of a membrane is essential for its operation when it is implemented at industrial scale. Concentration polarization and fouling change dynamically as a function of the time, making the outputs unsteady. Previously published literature on the topic lacks the insight of the adequate operating conditions on the performance and output of membranes. This aspect is of paramount importance in terms of productivity and target rejection efficiency for the process scale-up design and control. In all the tests carried out by these authors, the operating conditions remain fixed and do not report how these variables influence the rejection of the target species or the permeate flow and the behavior of the membrane concerning fouling. Also, the available scientific literature reports mainly membrane treatment processes for three-phase OMW, but there is a knowledge gap regarding OOWW of modern two-phase technology.

The challenge of the present work was to establish and control the operating framework and model the performance of the NF membrane operation. For this objective, a factorial design was used for the optimization of the process. The obtained results were interpreted through the response surface methodology. Statistical multifactorial analysis was performed to quantify all the potential complex conjugated effects of the input parameters considered in the NF process. Later, the process was modelled through a second-grade quadratic fitting model equation. Finally, the parametric quality standards that permit to reuse the purified stream for irrigation or in-site discharge and reuse purposes were checked. To the author's knowledge, no previous work on the optimization of membrane processes for OOWW purification and valorization can be found up to the present.

2. Experimental

2.1. The effluent stream: olive-oil-washing wastewater

Samples of OOWW were taken from two olive oil mills in the Andalusian provinces of Jaén ('Cooperativa San Ildefonso', Pegalajar) and Granada ('Aceites La Purísima', Alhendín) (South of Spain). These were modern mills operating with the most up-to-date two-phase olive oil production technology. Raw OOWW samples were taken directly from the vertical centrifuges in-situ during the olive oil production process. After collection, the raw OOWW was analyzed and directly used for the experiments, as fresh as it is by-produced, to avoid modifying its natural characteristics. Also, samples were kept under refrigeration ($-5\,^{\circ}C$) to maintain them stable for following experiments. The main physico-chemical characteristics of the raw OOWW samples are reported further in results and discussion section.

The treatment of the olive mill solid waste (OMSW) stream, commonly known as 'alpeorujo' (COD values up to $190\,g\,L^{-1}$) [25] out of the scope of this work, which is focused on the management problem of the liquid effluents' revalorization and reclamation. Some treatments proposed up to the current moment for the disposal of the olive pomace waste are composting [26] or biogas production [27], adsorption of heavy metals [28–30], dyes [31] and phenols [32], among others.

2.2. Determination of the point of zero charge of the NF membrane

The point of zero charge (PZC) of a membrane makes reference to the pH value upon which the membrane presents zero surface charge density. This is a consequence of equivalent amounts of negative and positive charges developed by proton equilibria. It is very relevant to determine the PZC of a corresponding membrane, since it will determine the intensity of the electrostatic interactions among the compounds present in the feedstream and the active surface of the

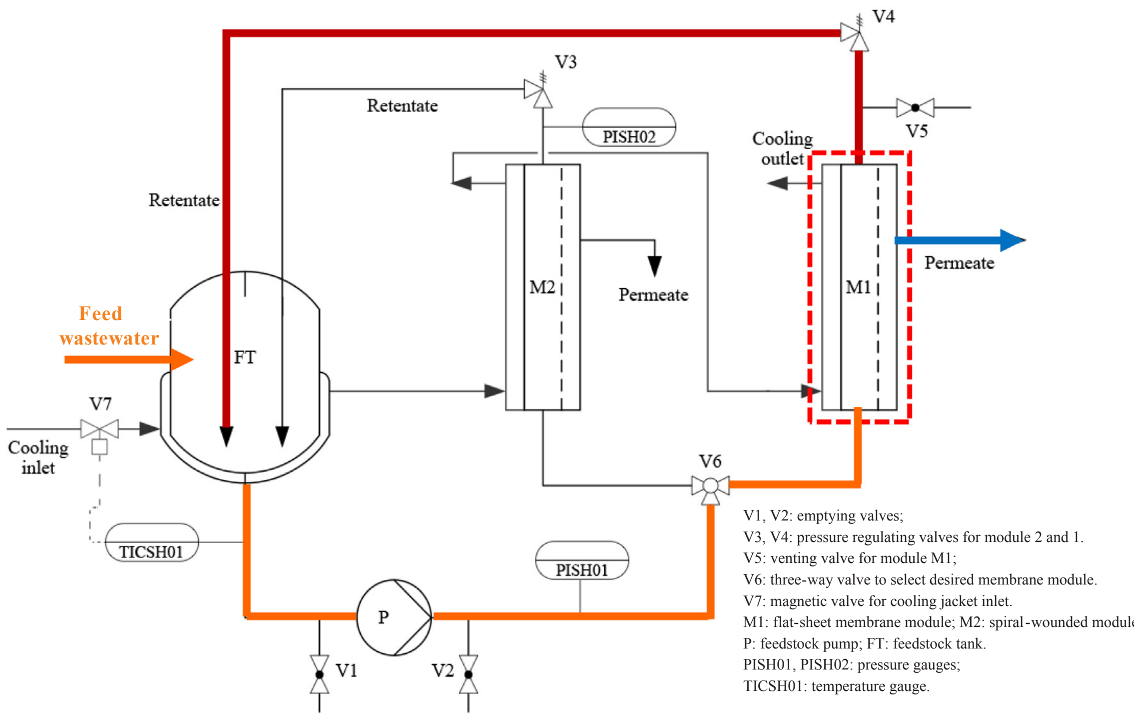

Fig. 1. Flow scheme of the bench-scale membrane unit.

membrane, thus having important effects on the membrane fouling – and thus flux – performance and rejection efficiency.

In this work, the PZC was determined by the procedure detailed by Mullet et al. [33]. This methodology consists in filtrating MilliQ® water solutions (18 MΩ cm) at different initial pH values (pH_0: 3.8, 5.5, 6.5 and 8.9) through the NF membrane in recirculation mode (tangential flow 2.55 m s^{-1}, minimum operating pressure allowable of the system 2.7 bar, and ambient temperature 22 ± 0.1 °C). The shift of the pH was registered (ΔpH) from the initial value until a stable value was attained. The PZC of the membrane was determined from the plot of ΔpH vs. pH_0, and corresponds to the point at which there is no variation of pH in the solution.

2.3. Membrane plant, NF membrane characteristics and experimental procedure

A bench-scale membrane plant (Prozesstechnik GmbH) was used for the experiments (flow scheme in Fig. 1). The full description of the system can be found in previous works by the authors [4,34]. Briefly, the system was equipped with a 5 L feed tank, provided with a temperature control jacket; a diaphragm pump (Hydra-Cell D-03) to carry the effluent (OOWW) into the desired membrane module – plate-and-frame module M1 in this study (3.9 cm height × 33.5 cm length × 14.2 cm width) – selectable with a three-way valve (V6).

The system was provided with all the necessary elements to measure, display and control the main operating variables: a digital pressure gauge (Ceraphant T PTC31, Endress + Hauser) to monitor and control the operating pressure (PISH01-02; $P_{TM\ set\ point}$ ± 0.01 bar) fixed by a spring-loaded pressure-regulating valve (V4) on the concentrate outlet (SS-R4512MM-SP, Swagelok); a flow-rate valve (0.1 L h^{-1}) to set the tangential velocity inside the module; a proportional-integral-derivative (PID) automatic electronic temperature controller (TICSH01; UT100, Yokogawa; $T_{set\ point}$ ± 0.1 °C), connected through a magnetic valve to a chiller (7306 model, PolyScience) to recirculate refrigerating or heating water into the jackets of the tank and modules. The bench plant was protected from overpressure and overtemperature automatically. The wetted metallic parts of the system were fabricated in 316L-stainless steel to avoid corrosion, whereas the permeate and concentrate tubes were made of chemically-resistant polyethylene. A thin-film composite (TFC) flat-sheet NF membrane of polyamide active layer on polysulfone ultrafiltration support (DK, GE Water & Process Technologies) was selected. The membrane was cut out from a larger roll, in flat-sheets (200 cm^2 active area). A polymeric net spacer (2 mm mesh diameter) was inserted into the plate-and-frame module to promote the appropriate turbulence to the feed over the membrane surface to minimize concentration polarization. The characteristics of the chosen membrane and spacer are reported in Table 1.

Before every experiment, the NF membrane was pre-conditioned by permeating reverse osmosis water (15 MΩ cm at 25 °C) under low pressure until the flux was stabilized (~2 h). Immediately after this, the pure water permeability of the membrane ($m_{w\ 22\pm0.5\ ^{\circ}C}$) was measured. Then, OOWW was introduced into the feed tank (600 mL) to begin the NF experiment in batch operation: the permeate stream was continuously collected (and stored for analysis) whilst the concentrate stream was steadily returned to the feed tank.

Rejection efficiencies were calculated with the following expression:

Table 1
Characteristics of the selected NF membrane and module spacer.

Parameters	Parametric value
Supplier	GE Water & Process Tech.
Model	DK
Active surface, m^2	0.02
Permeability (m_w), L h^{-1} m^{-2} bar^{-1}	6.49 ± 0.5
Configuration	Flat sheet
Chemical structure	Thin film composite (TFC)
Chemical composition	Polyamide/polysulfone
Surface nature	Hydrophilic
MWCO, Da	300
Average pore size, nm	0.5
Maximum pressure, bar	40
Maximum temperature, °C	50
pH range	1–11
Module spacer	Flat, 45 mil parallel

*MWCO: molecular weight cut off.

$$R_i(\%) = \left(1 - \frac{C_{p,i}}{C_{f,i}}\right) \times 100 \quad (1)$$

where $c_{p,i}$ is the concentration of the i species in the permeate stream, and $c_{f,i}$ is the concentration of the i species in the feedstream bulk.

The volume concentration factor (VCF), representing the ratio of final concentrate stream volume to initial feed effluent volume, was calculated as:

$$VCF = \frac{V_{initial}}{V_{concentrate}} \quad (2)$$

At the end of every NF run, the membrane was subjected to flushing with water (MilliQ®), in order to remove reversible fouling deposited on the membrane (flushing conditions: ambient temperature 25 °C, minimum system pressure 2.7 bar and turbulent tangential flow). Thereafter, the recovery of the membrane permeability (m_w) was checked (Rec_{rinsed}, %). If not fully restored, cleaning-in-place with NaOH and sodium dodecyl sulfate (SDS) (0.1–0.2% w/v) (Panreac S.A.) was performed to eliminate semi-reversible fouling to recover the membrane for following experiments (Rec_{final}, %) [34]. Rinsing with water was finally carried out to remove any remaining cleaning reagents from the system.

2.4. Process modelling

In order to optimize the NF process for OOWW valorization and purification, the statistical impact of the main operating variables – pressure (P), temperature (T), feed flow (F) or tangential flow velocity (v_t) and feedstream pH – on the membrane performance in terms of dynamic and steady-state permeate flux (Jp(t) and Jp_{ss}, $L\,h^{-1}\,m^2$) was examined.

To do this, statistical software *Statgraphics Centurion XV* was used to prepare a design of experiments (DDE). In this work, Box-Behnken design based on four factors was chosen. Box and Behnken [35] developed a family of efficient designs for factors with various levels that allow adjustment with quadratic models. It is a creative design based on the construction of incomplete balanced blocks. The design of Box-Behnken has a series of relevant characteristics, providing a sufficient number of profiles to test the goodness of the adjustment [35].

In our study, a series of values were assigned to the studied factors comprising 3 levels including a central point (0) and two equally-spaced extremes (± 1) (see Table 2). The model proposed the realization of 27 experiments, 3 of which correspond to the central point to ensure the reproducibility of the method.

In particular, the effluent pH was shifted from its raw pH_0 (5.13) to more acidic (3.63) or alkaline (7.63) conditions, which will lead to the development of different interactions with the NF membrane (below or above its PZC).

A temperature of 15 °C was set as minimum (−1), given the fact that it is in the range of the climatic conditions usually attained during the olive-oil production campaign (autumn-winter). Running the purification/valorization NF process at an operating temperature below this one would not be efficient from the point of view of the specific energy consumption, due to the amount of cold that would have to be supplied to the effluent to lower its temperature.

For the operating pressure, a maximum value (+1) of 35 bar was selected bearing in mind a necessary safety margin (δ) with respect to the maximum design pressure of the membrane (40 bar). The lowest pressure value (−1) was set at 15 bar, since working at lower pressures would entail very low permeate fluxes, even in some cases making filtration of OOWW impossible or economically unfeasible.

On another hand, for the tangential flow it was taken into account that it was high enough to cause turbulent flow at the inlet of the feedstream into the membrane module, measured by Reynolds number (N_{Re}). N_{Re} was calculated with the equation by Mott [36] for flow in rectangular sections:

$$N_{Re} = \frac{v(4R)\rho}{\mu} \quad (3)$$

where R corresponds to the hydraulic radius of the module, calculated as A/P in which A is the area (0.02 m^2) and P is the perimeter (0.68 m); v is the average speed of the fluid flow through the surface (that is, the tangential velocity v_t), ρ is the fluid density (kg/m^3) and μ is the fluid viscosity (kg/m s). The resulting v_t for the different volumetric flow values tested ($3{\cdot}10^{-5}$, $5{\cdot}10^{-5}$, and $7{\cdot}10^{-5}\,m^3/s$) were equal to 15, 25 and 35 $m\,s^{-1}$, which correspond to N_{Re} equal to $1.74{\cdot}10^6$, $2.90{\cdot}10^6$ and $4.06{\cdot}10^6$. As it can be noted, the flow regime promoted over the membrane was in the turbulent range, as per the N_{Re} obtained.

A statistical multifactorial analysis was implemented using the same software, with the aim of quantifying all possible complex conjugated effects of the input parameters considered in the OOWW NF purification process. Experimental results were interpreted by means of the response surface methodology (RSM). RSM consists in a series of mathematical and statistical technics for the collection of important quantity of information from the least number of data values that serve for process improvement and optimization. It can be used to evaluate the relative significance of diverse affecting factors. In this work, RSM was used to resolve the optimal operational conditions for the system and to define the region that complies with the operating specifications.

RSM method represents the system in the form of an empirical equation in which each particular coefficient is fitted based on the gathered data within the set of experiments carried out. Second order polynomial models including crossed terms that permit to describe satisfactorily the concavities or convexities of the surface are normally used. The ‘Response Surface’ represented by a polynomial model equation (Response Function, RF) comprising four variables is:

$$y = b_0 + b_1x_1 + b_2x_2 + b_3x_3 + b_4x_4 + b_{11}x_1^2 + b_{22}x_2^2 + b_{33}x_3^2 + b_{44} x_4^2 + b_{12}x_1x_2 + b_{13}x_1x_3 + b_{23}x_2x_3 + b_{34}x_3x_4 \quad (4)$$

where y represents the response function and x_1, x_2, x_3 and x_4 the input variables.

The resolution of the four-equational system permits to determine the values for the different input variables x_1, x_2, x_3 and x_4 for the optimal output point:

$$\frac{\delta y}{\delta x_i} = b_i + 2b_{ii}x_i + b_{ij}x_i = 0 \quad (5)$$

Finally, optimization and validation of the model was accomplished.

2.5. Analytical methods

Analyses of chemical oxygen demand (COD), total suspended solids (TSS), total phenolic compounds (TPhs), electrical conductivity (EC) and pH were performed in the raw effluent samples (OOWW) and in the permeate and concentrate streams of the NF membrane unit, following standard methods [25]. All analytical methods were triplicated and performed with analytical grade reagents (≥99% purity).

A Helios Gamma UV–visible spectrophotometer (Thermo Fisher Scientific) was used for COD and TPhs analyses. EC and pH were analyzed with a Crison GLP31 conductivity-meter and a Crison GLP21 pH-meter, provided with autocorrection of temperature (25 °C). The devices were previously calibrated with buffer standard solutions (Crison)

Table 2
Variables and ranges for analysis of variance (ANOVA) factorial design.

Variable	Minimum (−1)	Central (0)	Maximum (+1)
A: T, °C	15	22.5	30
B: P, bar	15	25	35
C: v_t, $m\,s^{-1}$	15	25	35
D: pH	3.63	5.13	7.63

for EC (1413 µS/cm and 12.88 mS/cm) and pH (4.01, 7.00 and 9.21).

TSS were determined by filtration of wastewater samples through a standard GF/F glass fiber filter. The residual retained on the filter was dried in an oven at 105 ± 1 °C until constant weight was attained. The increase in weight of the filter represents the total suspended solids [37].

COD was determined by photometric determination of chromium (III) concentration after 2 h oxidation with potassium dichromate/sulfuric acid/silver sulfate at 150 ± 0.5 °C (following standard methods DIN 38 409-H41-1 and DIN ISO 15 705-H45). Mercury sulfate previously was added to the samples to remove halides to avoid their interference in the COD measurement [37].

Phenolic compounds concentration (TPhs, in mg/L of equivalent gallic acid, GAE) was measured following Folin-Cicolteau method [37], with Folin-Cicolteau reagent (Sigma-Aldrich). This reagent contains sodic molybdate and tungstate (yellowish colour), which at basic pH react with any type of phenol, in a way that the transfer of electrons reduces phosphomolybdic-phosphotungstic complexes in tungsten and molybdenum oxides (W_8O_{23} and Mo_8O_{23}), being this proportional to the number of hydroxyl groups. The colour change into intense blue was then measured in the UV–visible spectrophotometer at 765 nm (Thermo Fisher Scientific).

3. Results and discussion

Engineering the design and operation of membrane plants at real industrial scale is a challenge in case of most purification processes, especially in wastewater treatment applications. The key for the feasibility of the process relies mainly on the accurate knowledge of the eventual interactions between the stream to be treated and the particular membrane selected, in order to control membrane fouling to be capable to run the process stably for long operating cycles without plant shut-downs [38–41].

Among the various factors that determine fouling phenomena, optimized operating conditions are of paramount relevance [38–41]. To this end, membrane engineers should minimize membrane fouling by operating membranes away from the permeate flux point upon which severe fouling is triggered. In many cases, if fouling effects are not well predicted and miss-estimated, the system will fail technically and economically in the short to medium run. On the other hand, modelling and optimization of the dynamic permeate flux can avoid excessive over-dimensioning of membrane necessities, which also result unfeasible as the fix costs are unnecessarily triggered.

3.1. OOWW main physico-chemical characteristics

The main physicochemical characteristics of the raw effluent (OOWW) are reported in Table 3. The effluent is characterized by a high COD and an acidic pH, as well as a valuable concentration of total phenolic compounds (TPhs) (~775.86 mg/L).

As it can be noted, lower COD is measured in two-phase OOWW liquid streams from vertical centrifuges if compared to three-phase OMW-3, which can rise up to 100,000 mg/L [1–4]. Nevertheless, the COD of OOWW is still very high to permit the discharge or reuse of this effluent for irrigation, and is therefore still a problem for this industry and the environment. In both cases, quantitatively the organic concentration would comprise fats and lipids, phenols, organic acids (which confer the acidic pH found), tannins and organohalogenated contaminants, which are mostly phytotoxic and thus recalcitrant to biological degradation. Because of the presence of still high COD and refractory compounds, direct disposal of these effluents to the municipal sewage treatment systems is currently banned.

Table 3
Main physicochemical characteristics of raw OOWW.

Parameter	Value
COD (mg/L)	13393.0–13964.5
TPhs (mg/L)	749.03–775.86
pH	5.10–5.25
EC (mS/cm)	1.82–2.10

EC: electrical conductivity; TPhs: total phenolic compounds.
*TSS: total suspended solids; COD: chemical oxygen demand.

Phenolic compounds are present in a wide variety of wastewaters, from olive mills, oil refineries, plastics, leather, paint, pharmaceutical and steel industries, as well as in domestic effluents and vegetation decay [38]. On one hand, if phenolic compounds are directly discharged into water bodies and land, they present high toxicity, refractoriness persistence and accumulation, thus representing an environmental issue. Within the current environmental regulations, these compounds must be eliminated before discharge of wastewater into water bodies or land, because of their prevalence in different wastewaters and their toxicity to living beings even at low concentrations.

Nevertheless, most phenolic compounds contain excellent antioxidant and radical scavenging properties, which can help eliminate free radicals in cells and thus enhance protection against oxidative stress in biomolecules comprising proteins, lipids and DNA, summed to antimicrobial and anticarcinogenic functions [39]. As a result, currently they are highly demanded in various industrial sectors, mainly cosmetic, pharmaceutical, biotechnological and food. A proof of this is their high market price, which on another hand is also inflated because up to the present these antioxidant compounds are commonly synthesized chemically.

3.2. Point of zero charge of the NF membrane

In this work, the method by Mullet et al. [33] was performed to determine the PZC of the NF membrane. Results are shown in Figs. 2 and 3. The methodology consists in circulating aqueous solutions (MilliQ® water) with different pH values through the membrane, and to record the pH changes (ΔpH) in the permeate from the initial value (pH_0) until a constant value is reached.

In Fig. 2, the evolution of pH in time of the different pH_0 solutions for PZC determination is reported. ΔpH equal to −0.25, −0.51, 0.83 and 2.79 were registered for the different solutions tested (pH_0: 3.8, 5.5, 6.5 and 8.9).

From the results obtained in the recirculation tests at different pH_0 values, the graph of pH variation (ΔpH) versus the initial pH (pH_0) for each solution was constructed. The ΔpH corresponds to the data once the steady state for each experiment was reached. The data of *ΔpH*

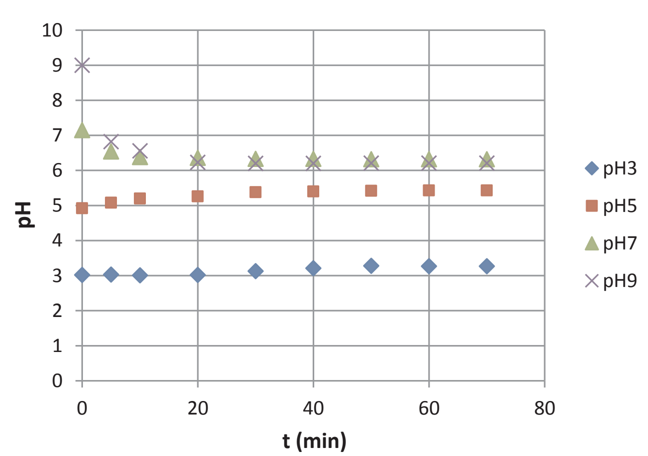

Fig. 2. pH value evolution in time of the different pH_0 solutions for PZC determination.

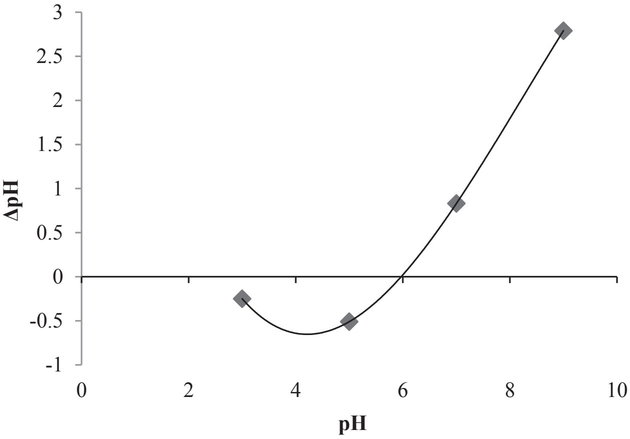

Fig. 3. Determination of the point of zero charge (PZC) of the NF membrane.

versus pH_0 are shown in Fig. 3. If the ΔpH observed experimentally is represented against the initial pH of the solution, the PZC of the membrane can be calculated, corresponding to the pH of the solution where ΔpH = 0, obtained by intersection of the ΔpH curve with x-axis (Fig. 3).

From the obtained results, it was determined that the point of zero charge (PZC) of the NF membrane (DK) is very close to 6 (PZC = 5.97), that is, it was found that the membrane presented zero surface charge density at a PZC value equal to 5.97. This would have non-negligible effects in the performance of the NF purification of OOWW, given that the membrane will have negative net surface charge density at pH above 5.97 (pH > PZC), whilst a positive surface charge would be developed below that point (pH < PZC).

This will be determinant regarding the intensity of the electrostatic interactions among the organic and inorganic species present in the OOWW stream, and between these and the active surface of the NF membrane, summed to the proper steric effects. The type and intensity of the attraction-repulsion interactions will affect the approach of the species to the interphase, hence modifying the rejection efficiency of the NF membrane and thus the fouling build-up, too. For pH values above the PZC of the membrane (ΔpH = PZC – pH < 0) the carboxyl groups of the active layer of the NF membrane will be deprotonated, and thus it will be negatively charged. However, for pH values below the zero charge point of the membrane (ΔpH > 0) the amino groups of the active layer of the NF membrane will be protonated and the membrane surface would be positively charged.

3.3. Membrane performance

The dynamic performance of the NF membrane upon the different operating conditions tested is given in detail in Fig. 4, where the permeate flux patterns during operation time (Jp(t) and Jp_{ss}, $L\,h^{-1}\,m^{-2}$) are shown.

Experimental results of the OOWW NF purification process are as well summarized in Table 4, in which the steady-state permeate flux values (Jp_{ss}) attained depending on the selected operating conditions are reported.

Results from the experiments performed highlight that maximum steady-state permeate flux was provided by the NF membrane under the following operational conditions: 35 °C, 25 bar, 35 $m\,s^{-1}$ and raw effluent pH (5.13), yielding a Jp_{ss} of 94.47, $L\,h^{-1}\,m^{-2}$. Also, upon the same temperature and pressure conditions but 35 $m\,s^{-1}$ and alkaline effluent pH (7.63), a second maximum Jp_{ss} equal to 90.59 $L\,h^{-1}\,m^{-2}$ could be attained. And a similar value, 88.0 $L\,h^{-1}\,m^{2}$, was obtained upon the same pressure and temperature, lower v_t (15 $m\,s^{-1}$) but upon the raw effluent pH.

Oppositely, the lowest permeate flux value (38.11 $L\,h^{-1}\,m^{-2}$) was registered upon 15 °C, 35 bar, 25 m/s and raw effluent pH (5.13). Also, upon 25 °C, 15 bar, 25 $m\,s^{-1}$ and alkaline effluent pH (7.63) a Jp_{ss} of 47.3 $L\,h^{-1}\,m^{-2}$ was measured, and very similarly, 47.94 $L\,h^{-1}\,m^{-2}$, upon 25 °C, 35 bar, 25 $m\,s^{-1}$ and acidified effluent pH (3.63).

For deeper understanding, the effects of each individual variable on the NF membrane performance during OOWW purification/valorization in terms of steady-state permeate flux (Jp_{ss}) are additionally shown in Fig. 5.

The variation of the steady-state permeate flux with the **operating pressure** presents a convex curve within the range of pressure values tested. A maximum permeate flux is appreciated when the pressure value is slightly above the central point (≈0.1), corresponding to 27–28 bar. At this pressure value the critical permeate flow is reached, and beyond this point the pressure ceases to be controlling, hence the control relies on the transfer of matter. Under operating pressure conditions higher than the critical point [40,41], the transport of particles towards the boundary region of the active layer of the membrane is so high that the balance between these and the repulsion force of the electric bilayer is exceeded, giving place to the deposition of particles on the surface of the membrane, therefore, to fouling of the membrane [40].

The variation of the tangential flow affected positively the permeate flux in almost directly proportional trend. The increase of the **flowrate** results in higher tangential velocity (v_t) on the surface of the membrane, observing in our case that higher v_t gives rise to a greater steady state permeate flow (Jp_{ss}). This results from the greater shear effect caused by the increase in turbulence at higher v_t on the membrane layer. This fact minimizes the formation of deposits on the membrane and at the same time allows a major drag force effect, reducing the fouling on the membrane.

The variation of **temperature** had practically a linear effect on the increase of the steady-state permeate flux value. By increasing the temperature from 15 °C to 35 °C, an increase of 36 $L\,h^{-1}\,m^{-2}$ was achieved. This fact has as a theoretical basis on the dissociation of organic matter present in the effluent to be filtered and a lower viscosity, forming aggregations of smaller particles and therefore a less dense fouling layer, giving rise to higher permeate flux. When the temperature increases, there is also a swelling effect of the membrane that favors the passage of solvent through it.

The effect of the **effluent pH** variation presents a concave curve with respect to the resulting permeate flux. A minimum flux is observed near the central point corresponding to the pH value of the sample (5.13), this point being very close to the PZC of the membrane (5.97). If the pH of the effluent is close to the PZC of the membrane, the existence of repulsion of one sign or another on the surface of the membrane will be practically zero, making the flow of permeate minimal. However, providing the effluent with a pH higher or lower than the PZC of the membrane will result in an increase in the permeate flow due to the net positive or negative charge created on the active layer of the membrane.

The VCF attained in this study was the maximum allowed by the bench-scale membrane equipment, taking in regard the dead-volume of the system. The higher the VCF, the higher would be the concentration of the solution fed to the NF system, and thus fouling on the membrane would be critical if the operating conditions are not properly optimized. In all the experiments performed, the volume of concentrate obtained was approximately equal to 80 mL, disregarding the experimental NF run conditions, resulting in VCF equal to:

$$VCF = \frac{V_{initial}}{V_{concentrate}} = \frac{520}{80} = 6.5$$

To sum up, the feedstream was concentrated up to 6.5 times the feedstream volume.

Otherwise, rinsing with deionized water performed at the end of every NF run permitted the assessment of the membrane permeability (m_w) recovery (Rec_{rinsed}, %) with respect to its initial value (m_{w0}). This

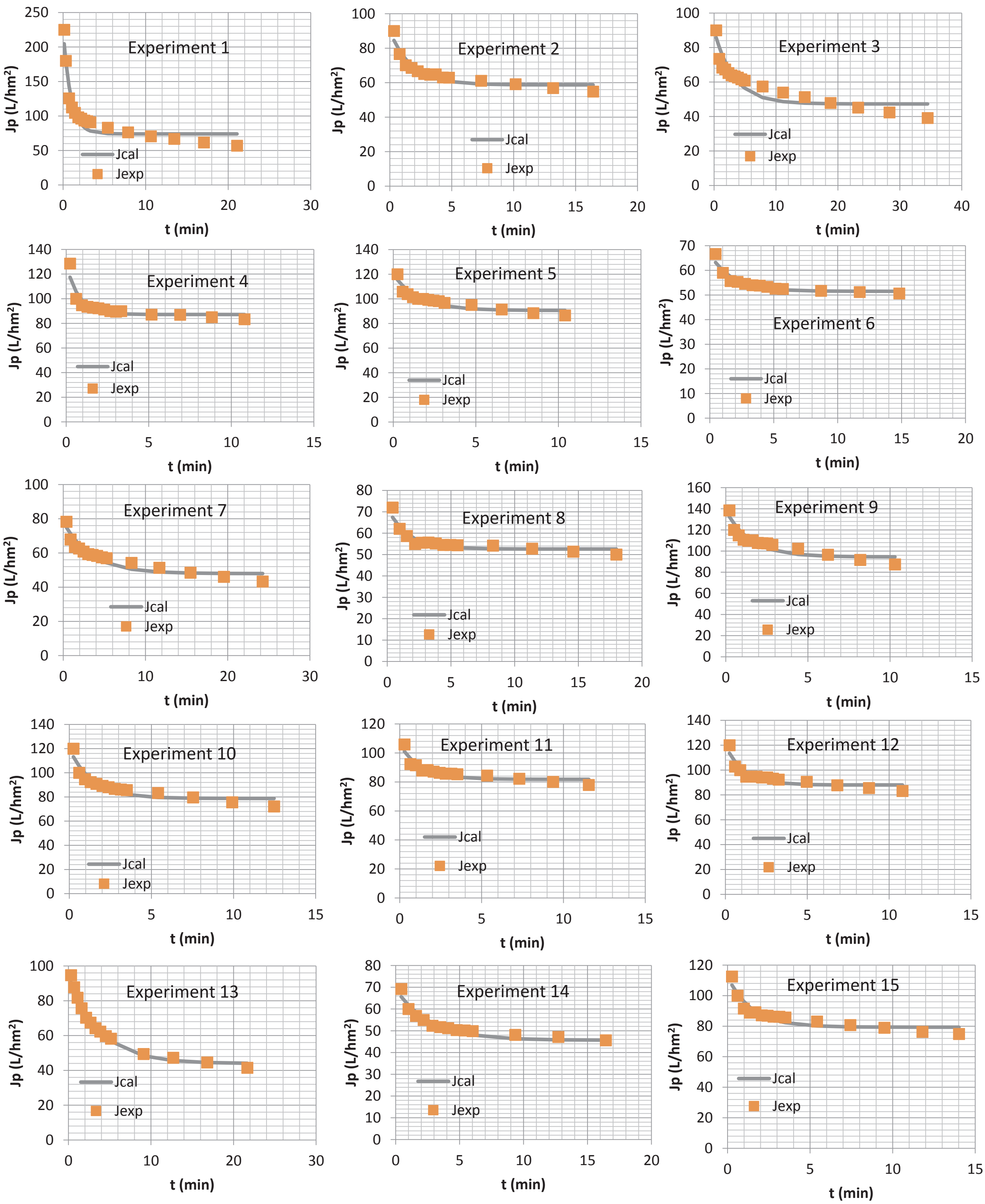

Fig. 4. Experimental NF permeate flux profiles.

permitted discerning the quantity of reversible fouling built-up on the NF membrane. After hydraulic cleaning (rinsing) of the NF membrane, it was possible to restore up to 83.20% of its permeability, which highlights that the majority of the permeate flux loss suffered by the NF membrane is the result of reversible fouling and concentration polarization.

On another hand, the soft chemical cleaning subsequently performed on the membrane allowed measuring again the membrane permeability to evaluate its recovery compared to the virgin membrane value (Rec_{final}, %), in order to determine semi-reversible membrane fouling. By performing this [42], the recovery of up to 98.4% of the membrane permeability was effective. Hence it can be confirmed that

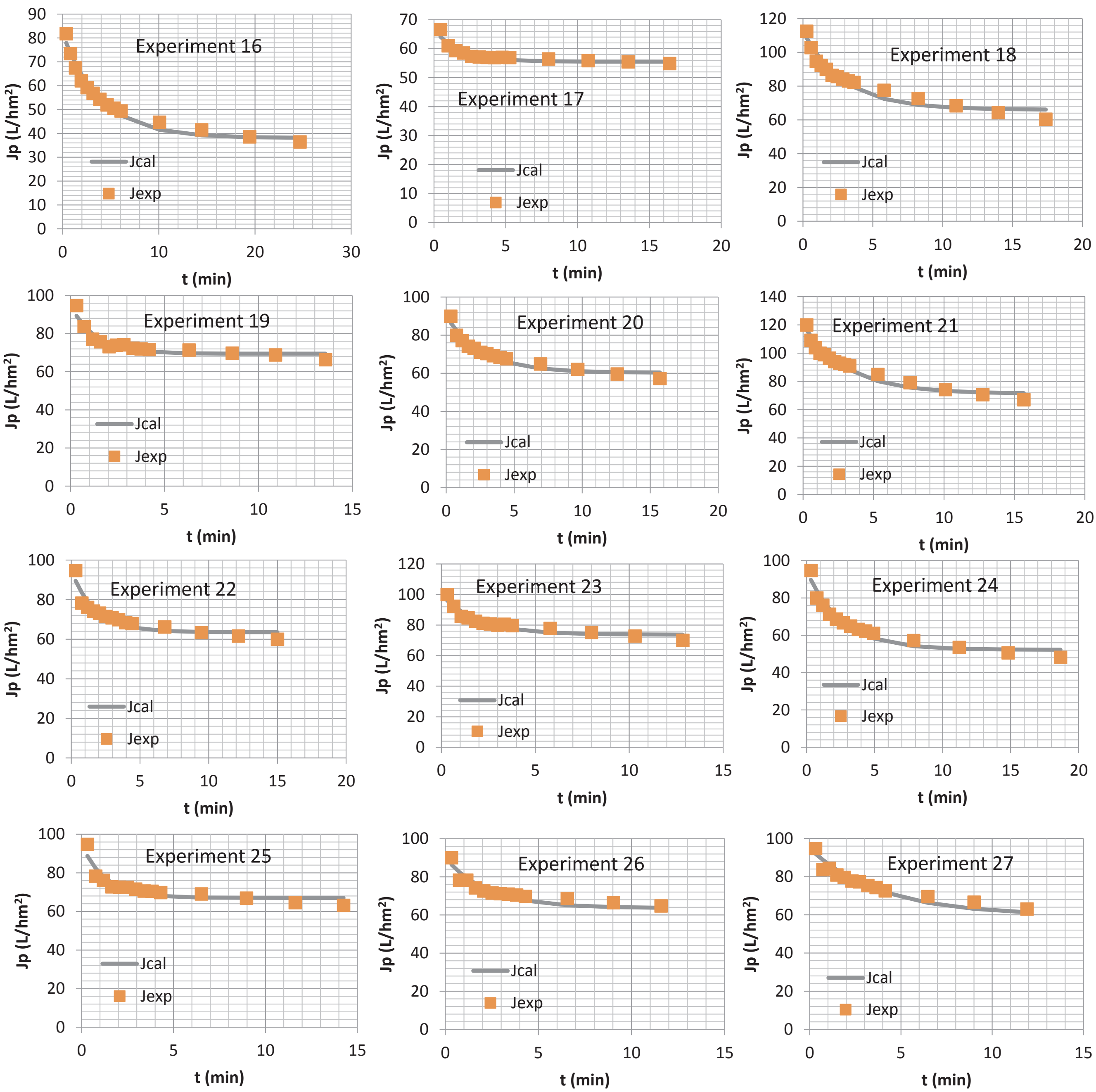

Fig. 4. (*continued*)

little amount of irreversible membrane fouling is built-up on the membrane, so the majority was of reversible and semi-reversible nature.

3.4. Statistical analysis and model development

Following the experimental results, *Statgraphics Centurion XV* software was used to carry out a statistical multifactorial analysis. The objective was to quantify the different complex and combined impacts of the input variables in the NF valorization/purification of OOWW, in order to statistically determine the operating conditions and squared effects that are significant and evaluate their relative impact in the response output (Jp_{ss}). The lower the p-value found, the higher significance of the impact of each individual factor on the response of the process (Jp_{ss}).

Results of the statistical analysis are reported in Table 5. The table of the ANOVA (Table 5) divides the variability of Jp_{ss} in separated pieces for every examined parameter. The statistical significance of each parameter is probed by comparing the mean squares with the experimental errors estimated. In accordance with the p-values statistically estimated for the different operating parameters of the NF process under study, reported in Table 5, it can be confirmed that all four input variables T, P, v_t and pH present a significant influence on the Jp_{ss} given by the membrane, as their p-value stands below 0.05. Therefore, it can be affirmed there is a statistically significant correlation among the examined variables at 95% confidence level.

Specifically, T and v_t exhibit the highest significance according to the p-values withdrawn from this analysis (p-values → 0), and also the squared effects of T, P and pH were found to be significant (p-values below 0.05). This can be graphically observed in the standarized Pareto chart in Fig. 6. In this chart, the effect on the response of the system, that is, the Jp_{ss} in $L\,h^{-1}\,m^{-2}$ is quantified and represented, indicating if

Table 4
Results of randomized OOWW NF valorization and purification experiments.

Experiment	T, °C	P, bar	v_t, m s^{-1}	pH	Jp_{ss}, L h^{-1} m^{-2}
1	35	25	25	3.63	74.02
2	15	25	15	5.13	58.72
3	25	15	25	7.63	47.30
4	35	15	25	5.13	87.17
5	**35**	**25**	**25**	**7.63**	**90.59**
6	25	15	15	5.13	51.50
7	25	35	25	3.63	47.94
8	25	25	15	3.63	52.60
9	**35**	**25**	**35**	**5.13**	**94.47**
10	35	35	25	5.13	78.76
11	25	25	15	7.63	81.82
12	**35**	**25**	**15**	**5.13**	**88.00**
13	25	15	25	3.63	43.97
14	15	15	25	5.13	45.66
15	25	25	35	7.63	79.33
16	15	35	25	5.13	38.11
17	25	15	35	5.13	55.53
18	25	25	35	3.63	66.01
19	25	35	15	5.13	69.50
20	15	25	25	7.63	60.33
21	25	35	35	5.13	71.38
22	15	25	35	5.13	63.56
23	25	35	25	7.63	73.74
24	15	25	25	3.63	52.26
25	25	25	25	5.13	67.00
26	25	25	25	5.13	63.62
27	25	25	25	5.13	59.74

Maximum values attained are in bold.

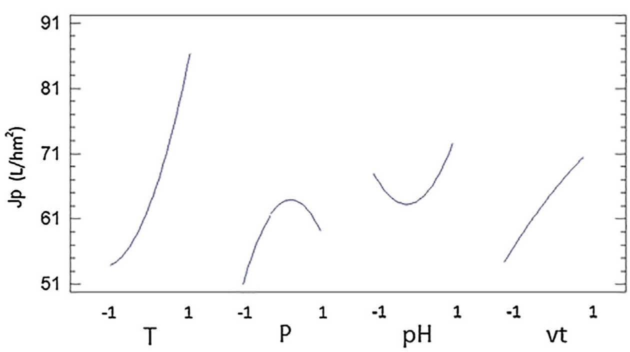

Fig. 5. Main effects of the operating variables (T, P, pH and v_t) on the steady-state permeate flux (Jp_{ss}, L h^{-1} m^{-2}).

Table 5
Analysis of variance (ANOVA) of Box-Behnken design (BBD).

Source	Sum of square (SS)	Degree of freedom (DF)	Mean square (MS)	F-ratio	p-value
A: **T**	3148.31	1	3148.31	63.87	**0.0000**
B: P	194.408	1	194.408	3.94	0.0704
C: pH	65.9883	1	65.9883	1.34	0.2698
D: $\mathbf{v_t}$	772.968	1	772.968	15.68	**0.0019**
AA	240.725	1	240.725	4.88	**0.0473**
AB	0.1849	1	0.1849	0.00	0.9522
AC	0.664225	1	0.664225	0.01	0.9095
AD	18.0625	1	18.0625	0.37	0.5562
BB	377.927	1	377.927	7.67	**0.0170**
BC	1.15562	1	1.15562	0.02	0.8809
BD	126.225	1	126.225	2.56	0.1355
CC	247.672	1	247.672	5.02	**0.0447**
CD	63.2025	1	63.2025	1.28	0.2796
DD	5.32445	1	5.32445	0.11	0.7481
Pure error	591.543	12			
Total error	6267.6	26			

Maximum values attained are in bold.

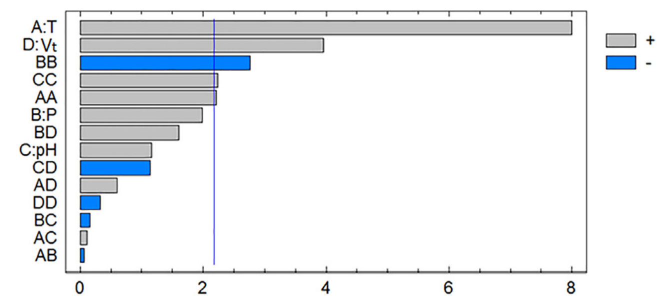

Fig. 6. Standarized Pareto chart for the OOWW NF valorization/purification process: effect of the operating variables – T (A), P (B), pH (C) and v_t (D) – and squared effects.

its magnitude is or not significant. The data withdrawn (Table 5) support the correctness of the proposed model as a function of all T, P, pH and v_t.

On another hand, the effects of terms B, C, AB, AC, AD, BC, BD, CD and DD were found not to be significant at 95% level, and therefore were eliminated from the model equation. These levels of impact are also graphically reported for ease of comprehension in the Pareto Chart given in Fig. 6. This diagram shows which response variables have a positive or negative effect on the permeate flux of the NF membrane. The vertical dividing line shows the variables that are not significant (they remain to the left of the line) and those that are significant (they surpass the line), under an imposition of a p-value of 0.05.

The definite second-grade quadratic fitting model equation obtained from the correlation among the theoretical values of the parameters and the operating conditions determined by multiple non-linear regression analysis was the following one:

$$Jp_{ss}, \text{L h}^{-1}\text{m}^{-2} = 63.4533 + 16.1975 \cdot T + 8.02583 \cdot v_t + 6.71833 \cdot T^2 - 8.41792 \cdot P^2 + 6.81458 \cdot pH^2$$

The statistic R^2 indicates that the fitting model equation can explain up to 90.5619% of the variability in the Jp_{ss} (Table 5). Moreover, from the ANOVA analysis derives a p-value of 0.01 for the model. Given that this value is below 0.05 it can be concluded that there is a significant relationship among Jp_{ss} and T, P, v_t and pH parameters in the form specified by the model considered at the 95.0% confidence level.

The estimated standard error points that the standard deviation of the residues is 7.021, and a mean absolute error (MAE) of the residues of 3.689. The Durbin-Watson statistic was 2.204 (p-value = 0.6892). Given that this value was very close to 2, this confirms that the residuals vary randomly and there is no indication of serial autocorrelation among them at 95.0% confidence level. In addition to this, the p-value higher than 0.05 indicates that there is no correlation at the 5% significance level. Also, the Lag 1 residual autocorrelation was found to be −0.115 (Table 5), a value near to zero which means that there is not significant structure unaccounted by the proposed statistical model.

3.5. Response surfaces and process optimization

Results derived from the process modelling were interpreted by means of the response surface methodology. The contour plots and response surfaces obtained for the proposed NF OOWW valorization/purification process are hereafter shown in Fig. 7. These response surfaces and contour plots support the data previously gathered and discussed by non-linear multifactorial regression analysis.

In these figures, the effect of each pair of variables on the NF system response, in terms of Jp_{ss} (L h^{-1} m^{-2}), is graphically shown: the contour plots (right figures) mirror the patterns of the response surfaces (left ones), with the only difference that the data are shown in form of upper or lower bounds, where the maximum region is marked with a cross ($^+$). The existence of a critical flux value as a function of the

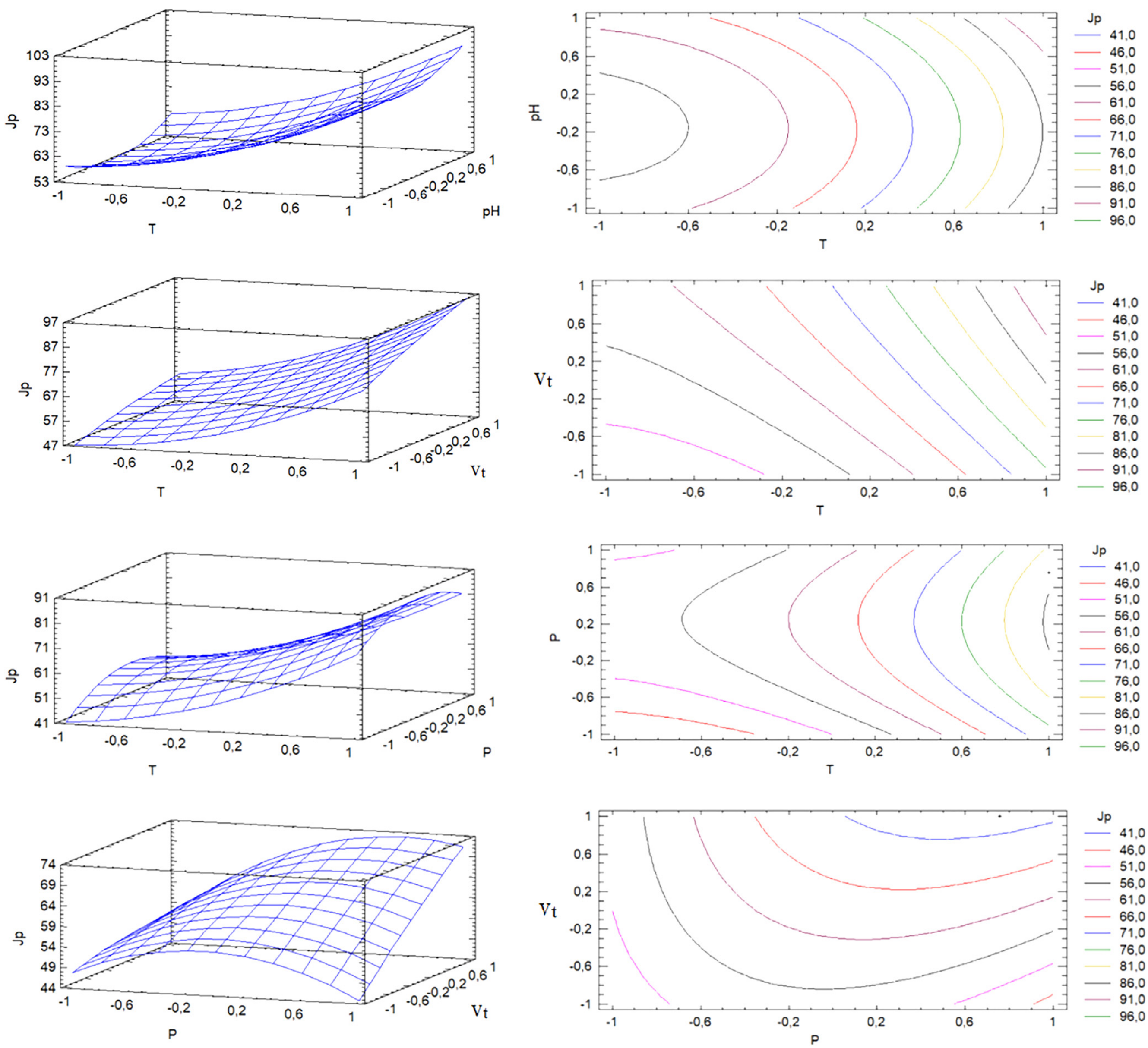

Fig. 7. Response surfaces (left side) and contour plots (right side): effect of the operating variables – T (A), P (B), pH (C) and v_t (D).

operating pressure (P vs. T and P vs. v_t) can be clearly seen in Fig. 7 [41,43]. This supports the key relevance of the boundary flux-pressure conditions on the performance of the membrane, as highlighted in previous works by the Stoller and Ochando [41], based on prior observations by Field et al. [40]. On another hand, a focus on Fig. 7 allows noting a maximum stable permeate flux attained by the NF membrane at the highest and lowest pH values, that is, above or below the PZC. Within these conditions, a plateau was quickly developed during the course of the operation, indicating minimum fouling on the NF membrane. Under alkaline pH conditions of the OOWW feedstream in contact with the membrane surface, deprotonation equilibria of carboxylic functional groups on the active layer of the membrane increase with the pH, hence the electronegativity of the NF membrane. As a consequence, the repulsion among the organic molecules in OOWW, which present mostly negative charge at those pH values, and the membrane surface becomes enhanced. Similarly occurred during the runs at low effluent pH, owed to the protonation of the amino groups on the membrane layer that provides it with a net positive charge.

On the other contrary, when the gap between the pH of the feedstream (OOWW) and the membrane PZC (PZC = 5.97) is narrowed, the Jp_{ss} provided by the NF membrane is reduced. In fact, the permeate flux during NF operation decreases steadily in time. In these conditions, the pH of the effluent is close to the PZC of the membrane, the absence of electrostatic repulsion among the organic species in the feedstream and the active layer of the membrane (Donnan exclusion) enhances deposition and fouling-build-up mechanisms [33]. Hydrophilic organic matter and colloidal pollutants of OOWW, mainly phenolic compounds and carboxylic organic acids [44], become protonated and hence neutrally charged at acid pH values (pH < PZC). These facts enhance deposition and accumulation of particles on the NF membrane surface if it is not charged, triggering fouling [40–44]. Hence, providing the system with a pH below or above the PZC of the membrane would result in an increase in the permeate flux due to the net positive or negative charge attained on the active layer of the membrane.

To sum up, the results of the optimization of the OOWW NF valorization/purification process are briefly reported in Table 6. These results support those found previously in the examination of the operating variables effect on the NF process performance and confirm the good agreement between experimental and predicted values. The optimized parameters for the proposed OOWW purification process were

Table 6
Optimized parameters values for the NF purification process of OOWW stream.

Factor	T, °C	P, bar	pH	v_t, m s^{-1}	Predicted final Jp_{ss}, L h^{-1} m^{-2}	R-Square (R^2)
Optimal value	35	26.5	3.7	32.7	106.14	90.5619
Optimal range	30–35	25–26.5	3.7–5.1	32.7–35	94.5–106.14	90.5619

estimated to be an operating pressure of 26.5 bar, tangential velocity 32.7 m s^{-1}, system temperature 35 °C and pH equal to 3.7. These conditions ensured a high and stable Jp_{ss} up to 106.2 L h^{-1} m^{-2}. If compared to obtained results in which the direct treatment of the raw effluent by NF yielded sensibly lower flux productivity, 44.6 L h^{-1} m^{-2}, this means a sensible increment of the permeate flux of the selected NF membrane as high as 58%.

This would have an important impact in the proposed NF membrane process for OOWW valorization and purification from a cost-efficiency point of view, given that the examined NF membrane was highly efficient (~106.2 L h^{-1} m^{-2}) at ambient temperature conditions, which is very relevant since the operating temperature is a key variable from a technical-economical point of view. Therefore, the effluent could be straightly driven from the outlet of the vertical centrifuges in the mills at their exiting temperature directly to the NF membrane, without the need of heating or cooling, enhancing the economic feasibility of the proposed process. Furthermore, this fact meets the need to not overcome the temperature point (T ≥ 35 °C) at which phenolic compounds begin to be degraded, thus avoiding any loss of added-value compounds. In addition to this, no acidification or basification of the effluent would be needed, since the improvement in terms of permeate flux attained on the NF membrane upon acidifying the OOWW feedstream is marginal if compared to the results (~94.5 L h^{-1} m^{-2}) provided with the raw effluent (pH = 5.13). As reported in these figures, high and steady permeate flux can be yielded within the ambient temperature range (30–35 °C), medium operating pressure (25–26.5 bar), raw pH (3.7–5.1) and turbulent crossflow (32.7–35 m s^{-1}).

The obtained results show that the optimization of the operation variables lead to the obtention of a highly efficient productivity of the membrane, since the permeate flux value is very high and stable during the operation of the membrane. This highlights a low fouling index, which is the key to extend the service-lifetime of the membrane, as well as to minimize the frequency of stops to carry out the cleaning of the membrane, with the consequent saving, both economic and environmental, of the reagents consumption. After the hydraulic cleaning of the NF membrane, it was possible the recovery of 87.6% of its permeability, pin-pointing that most permeate flux loss by the NF membrane within the optimized operating conditions is due to reversible fouling and concentration polarization. In addition, in these conditions the soft cleaning protocol could effectively recover steadily 99.8–100% of the membrane permeability, confirming that irreversible membrane fouling was negligible if the NF membrane operation is properly optimized. This would enhance the membrane lifetime and thus the feasibility of the integral process proposed.

Finally, under the optimized conditions, measured rejection of COD, EC and TPhs was above 86.8%, 40.9% and 95.1%, which would permit obtaining a permeate stream that could be reused for irrigation purposes, while the retantate stream was concentrated in volume up to 6.5 times, with a total phenolic content of minimum 1315.7 mg/L.

4. Conclusions

In the present research paper the optimization and modelling of an environmentally friendly NF process for the treatment and valorization of the wastewater streams produced in two-phase olive-oil mills (OOWW) is reported. The optimized parameters for the proposed OOWW purification process – operating pressure of 26.5 bar, tangential velocity 32.7 m s^{-1}, system temperature 35 °C and pH of 3.7 – ensured very high and stable flux of the membrane, up to 106.2 L h^{-1} m^{-2}. This represents 58% increment of the membrane productivity if compared to non-optimized NF procedure.

The obtained optimized data are very relevant for the feasible scale-up of the proposed process in the mills, since the NF membrane was highly efficient at ambient temperature conditions and raw effluent pH. This would mean that the effluent could be driven directly from the outlet of the vertical centrifuges at their exiting temperature to the NF membrane, without heating or cooling, enhancing the cost-efficiency of the proposed process. Moreover, this would also mean working at a temperature below the point at which phenolic compounds begin to be degraded, avoiding the loss of these added-value compounds. Also, no acidification or basification of the feed would be necessary, since the improvement in terms of permeate flux attained on the NF membrane upon modifying the OOWW feedstream pH is marginal if compared to the results provided with the direct use of the raw effluent (~94.5 L h^{-1} m^{-2}). Finally, the optimized conditions provided a permeate stream that could be reused for irrigation purposes and a retantate stream concentrated in volume up to 6.5 times, with a total phenolic content above 1315.7 mg/L.

Declaration of Competing Interest

Authors declare no conflict of interests.

Acknowledgements

Spanish Ministry of Economy and Competitiveness is acknowledged for having funded the project CTM2014-61105-JIN '*Design and development of an integral process for revalorization and treatment of the effluents from olive oil industry*', as well as the University of Granada.

References

[1] M. Niaounakis, C.P. Halvadakis, Olive Processing Waste Management: Literature Review and Patent Survey, Elsevier, 2006.
[2] P. Paraskeva, E. Diamadopoulos, Technologies for olive mill wastewater (OMW) treatment: a review, J. Chem. Technol. Biotechnol. 81 (2006) 1475–1485, https://doi.org/10.1002/jctb.1553.
[3] J.M. Ochando-Pulido, S. Pimentel-Moral, V. Verardo, A. Martinez-Ferez, A focus on advanced physico-chemical processes for olive mill wastewater treatment, Sep. Purif. Technol. 179 (2017) 161–174, https://doi.org/10.1016/j.seppur.2017.02.004.
[4] J.M. Ochando-Pulido, G. Hodaifa, M.D. Victor-Ortega, S. Rodriguez-Vives, A. Martinez-Ferez, Reuse of olive mill effluents from two-phase extraction process by integrated advanced oxidation and reverse osmosis treatment, J. Hazard. Mater. 263, Part 1 (2013) 158–167.
[5] J.M. Ochando-Pulido, R. González-Hernández, A. Martinez-Ferez, On the effect of the operating parameters for two-phase olive-oil washing wastewater combined phenolic compounds recovery and reclamation by novel ion exchange resins, Sep. Purif. Technol. 195 (2018) 50–59, https://doi.org/10.1016/j.seppur.2017.11.075.
[6] J.M. Ochando-Pulido, M. Stoller, A. Martinez-Ferez, Boundary flux modelling for purification optimization of differently-pretreated agro-industrial wastewater with nanofiltration, Sep. Purif. Technol. 193 (2018) 147–154, https://doi.org/10.1016/j.seppur.2017.10.071.
[7] I. Karaouzas, N.T. Skoulikidis, U. Giannakou, T.A. Albanis, Spatial and temporal effects of olive mill wastewaters to stream macroinvertebrates and aquatic ecosystems status, Water Res. 45 (2011) 6334–6346, https://doi.org/10.1016/j.watres.2011.09.014.
[8] G. Hodaifa, J.M. Ochando-Pulido, S. Rodriguez-Vives, A. Martinez-Ferez, Optimization of continuous reactor at pilot scale for olive-oil mill wastewater treatment by Fenton-like process, Chem. Eng. J. 220 (2013) 117–124, https://doi.org/10.1016/j.cej.2013.01.065.
[9] S. Ntougias, F. Gaitis, P. Katsaris, S. Skoulika, N. Iliopoulos, G.I. Zervakis, The

effects of olives harvest period and production year on olive mill wastewater properties - Evaluation of Pleurotus strains as bioindicators of the effluent's toxicity, Chemosphere 92 (2013) 399–405, https://doi.org/10.1016/j.chemosphere.2013.01.033.

[10] A.C. Barbera, C. Maucieri, V. Cavallaro, A. Ioppolo, G. Spagna, Effects of spreading olive mill wastewater on soil properties and crops, a review, Agric. Water Manag. 119 (2013) 43–53, https://doi.org/10.1016/j.agwat.2012.12.009.

[11] G. Mustafa, K. Wyns, A. Buekenhoudt, V. Meynen, Antifouling grafting of ceramic membranes validated in a variety of challenging wastewaters, Water Res. 104 (2016) 242–253, https://doi.org/10.1016/j.watres.2016.07.057.

[12] L.C. Davies, A.M. Vilhena, J.M. Novais, S. Martins-Dias, Olive mill wastewater characteristics: modelling and statistical analysis, Grasas Aceites 55 (2004) 233–241, https://doi.org/10.3989/gya.2004.v55.i3.171.

[13] A. Bódalo-Santoyo, J.L. Gómez-Carrasco, E. Gómez-Gómez, F. Máximo-Martín, A.M. Hidalgo-Montesinos, Application of reverse osmosis to reduce pollutants present in industrial wastewater, Desalination 155 (2003) 101–108, https://doi.org/10.1016/S0011-9164(03)00287-X.

[14] J. Luo, L. Ding, Y. Wan, M.Y. Jaffrin, Threshold flux for shear-enhanced nanofiltration: experimental observation in dairy wastewater treatment, J. Membr. Sci. 409–410 (2012) 276–284, https://doi.org/10.1016/j.memsci.2012.03.065.

[15] D.P. Zagklis, A.I. Vavouraki, M.E. Kornaros, C.A. Paraskeva, Purification of olive mill wastewater phenols through membrane filtration and resin adsorption/desorption, J. Hazard. Mater. 285 (2015) 69–76, https://doi.org/10.1016/j.jhazmat.2014.11.038.

[16] J.M.O. Pulido, A review on the use of membrane technology and fouling control for olive mill wastewater treatment, Sci. Total Environ. 563–564 (2016) 664–675, https://doi.org/10.1016/j.scitotenv.2015.09.151.

[17] J.M. Ochando-Pulido, V. Verardo, A. Segura-Carretero, A. Martinez-Ferez, Technical optimization of an integrated UF/NF pilot plant for conjoint batch treatment of two-phase olives and olive oil washing wastewaters, Desalination 364 (2015) 82–89, https://doi.org/10.1016/j.desal.2014.10.040.

[18] M. Stoller, A three year long experience of effective fouling inhibition by threshold flux based optimization methods on a nf membrane module for olive mill wastewater treatment, Chem. Eng. Trans. 32 (2013) 37–42, https://doi.org/10.3303/CET1332007.

[19] M.A. Saad, Membrane desalination for the Arab world: overview and outlook, Arab Water World. 1 (2005) 10–14.

[20] M. Stoller, B. De Caprariis, A. Cicci, N. Verdone, M. Bravi, A. Chianese, About proper membrane process design affected by fouling by means of the analysis of measured threshold flux data, Sep. Purif. Technol. 114 (2013) 83–89, https://doi.org/10.1016/j.seppur.2013.04.041.

[21] M. Stoller, J.M. Ochando-Pulido, L. Di Palma, A. Martínez-Férez, Membrane process enhancement of 2-phase and 3-phase olive mill wastewater treatment plants by photocatalysis with magnetic-core titanium dioxide nanoparticles, J. Ind. Eng. Chem. 30 (2015) 147–152.

[22] M. Stoller, R. Serrão Mendes, Advanced control system for membrane processes based on the boundary flux model, Separ. Purif. Technol. 175 (2017) 527–535.

[23] G. Di Lecce, A. Cassano, A. Bendini, C. Conidi, L. Giorno, T. Gallina-Toschi, Characterization of olive mill wastewater fractions treatment by integrated membrane process, J. Sci. Food Agric. 94 (2014) 2935–2942.

[24] E. Garcia-Castello, A. Cassano, A. Criscuoli, C. Conidi, E. Drioli, Recovery and concentration of polyphenols from olive mill wastewaters by integrated membrane system, Water Res. 44 (2010) 3883–3892.

[25] R. Borja, F. Raposo, B. Rincón, Treatment technologies of liquid and solid wastes from two-phase olive oil mills, Grasas y Aceites: Int. J. Olive Oil 57 (1) (2006) 32–46.

[26] M.S.Y. Haddadin, J. Haddadin, O.I. Arabiyat, B. Hattar, Biological conversion of olive pomace into compost by using Trichoderma harzianum and Phanerochaete chrysosporium, Biores. Tech. 100 (20) (2009) 4773–4782.

[27] A.R. Tekin, A. Coskun Dalgıc, Biogas production from olive pomace, Resour. Conserv. Recy. 30 (4) (2000) 301–313.

[28] R. Baccar, J. Bouzid, M. Feki, A. Montiel, Preparation of activated carbon from Tunisian olive-waste cakes and its application for adsorption of heavy metal ions, J. Hazard. Mater. 162 (2–3) (2009) 1522–1529.

[29] E. Malkoc, Y. Nuhoglu, M. Dundar, Adsorption of chromium (VI) on pomace –An olive oil industry waste: batch and column studies, J. Hazard. Mater. 138 (1) (2006) 142–151.

[30] J. Bouzid, Z. Elouear, M. Ksibi, M. Feki, A. Montiel, A study on removal characteristics of copper from aqueous solution by sewage sludge and pomace ashes, J. Hazard. Mater. 152 (2) (2008) 838–845.

[31] T. Akar, I. Tosun, Z. Kaynak, E. Ozkara, O. Yeni, E.N. Sahin, S.T. Akar, An attractive eagro-industrial by-product in environmental cleanup: dye biosorption potential of untreated olive pomace, J. Hazard. Mater. 166 (2–3) (2009) 1217–1225.

[32] A.S. Stasinakis, I. Elia, A.V. Petalas, C.P. Halvadakis, Removal of total phenols from olive-mill wastewater using an agricultural by-product, olive pomace, J. Hazard. Mater. 160 (2–3) (2008) 408–413.

[33] M. Mullet, P. Fievet, A. Szymczyk, A. Foissy, J.-C. Reggiani, J. Pagetti, A simple and accurate determination of the point of zero charge of ceramic membranes, Desalination 121 (1999) 41–48, https://doi.org/10.1016/S0011-9164(99)00006-5.

[34] J.M. Ochando-Pulido, M.D. Victor-Ortega, A. Martínez-Ferez, On the cleaning procedure of a hydrophilic reverse osmosis membrane fouled by secondary-treated olive mill wastewater, Chem. Eng. J. 260 (2015) 142–151, https://doi.org/10.1016/j.cej.2014.08.094.

[35] G.E.P. Box, D.W. Behnken, Some new three level designs for the study of quantitative variables, Technometrics. 2 (1960) 455–475, https://doi.org/10.1080/00401706.1960.10489912.

[36] R.L. Mott, J.A. Untener, Applied Fluid Mechanics, seventh ed., Pearson Prentice Hall, 2006.

[37] A.E. Greenberg, L.S. Clesceri, A.D. Eaton, Standard Methods for Examination of Water and Wastewate, 22nd ed., APHA/AWWA/WEF, Washington DC. Cabs, 2005.

[38] M. Pizzichini, C. Russo, C.D. Di Meo, Purification of pulp and paper wastewater, with membrane technology, for water reuse in a closed loop, Desalination 178 (2005) 351–359, https://doi.org/10.1016/j.desal.2004.11.045.

[39] R.W. Field, J.J. Wu, Modelling of permeability loss in membrane filtration: re-examination of fundamental fouling equations and their link to critical flux, Desalination 283 (2011) 68–74, https://doi.org/10.1016/j.desal.2011.04.035.

[40] R.W. Field, G.K. Pearce, Critical, sustainable and threshold fluxes for membrane filtration with water industry applications, Adv. Colloid Interface Sci. 164 (2011) 38–44, https://doi.org/10.1016/j.cis.2010.12.008.

[41] M. Stoller, J.M. Ochando-Pulido, The Boundary Flux Handbook: A Comprehensive Database of Critical and Threshold Flux Values for Membrane Practitioners, 2014. doi:10.1016/C2014-0-00504-7.

[42] X. Wei, Z. Wang, F. Fan, J. Wang, S. Wang, Advanced treatment of a complex pharmaceutical wastewater by nanofiltration: membrane foulant identification and cleaning, Desalination. 251 (2010), https://doi.org/10.1016/j.desal.2009.08.005.

[43] M. Stoller, J.M. Ochando-Pulido, Going from a critical flux concept to a threshold flux concept on membrane processes treating olive mill wastewater streams, 2012, pp. 607–608. doi:10.1016/j.proeng.2012.08.500.

[44] J.M. Ochando-Pulido, A. Martinez-Ferez, A focus on pressure-driven membrane technology in olive mill wastewater reclamation: state of the art, Water Sci. Technol. 66 (2012) 2505–2516, https://doi.org/10.2166/wst.2012.506.